RSC Chemical Biology

ROYAL SOCIETY OF CHEMISTRY

COMMUNICATION

View Article Online
View Journal | View Issue

Cite this: *RSC Chem. Biol.*, 2023, 4, 884

Received 29th June 2023,
Accepted 25th September 2023

DOI: 10.1039/d3cb00110e

rsc.li/rsc-chembio

Evaluation of Kdo-8-N_3 incorporation into lipopolysaccharides of various *Escherichia coli* strains†

Zeynep Su Ziylan,[a] Geert-Jan de Putter,[a] Meike Roelofs,[a] Jan Maarten van Dijl,[b] Dirk-Jan Scheffers[c] and Marthe T. C. Walvoort*[a]

8-Azido-3,8-dideoxy-α/β-D-*manno*-oct-2-ulosonic acid (Kdo-8-N_3) is a Kdo derivative used in metabolic labeling of lipopolysaccharide (LPS) structures found on the cell membrane of Gram-negative bacteria. Several studies have reported successful labeling of LPS using Kdo-8-N_3 and visualization of LPS by a fluorescent reagent through click chemistry on a selection of Gram-negative bacteria such as *Escherichia coli* strains, *Salmonella typhimurium*, and *Myxococcus xanthus*. Motivated by the promise of Kdo-8-N_3 to be useful in the investigation of LPS biosynthesis and cell surface labeling across different strains, we set out to explore the variability in nature and efficiency of LPS labeling using Kdo-8-N_3 in a variety of *E. coli* strains and serotypes. We optimized the chemical synthesis of Kdo-8-N_3 and subsequently used Kdo-8-N_3 to metabolically label pathogenic *E. coli* strains from commercial and clinical origin. Interestingly, different extents of labeling were observed in different *E. coli* strains, which seemed to be dependent also on growth media, and the majority of labeled LPS appears to be of the 'rough' LPS variant, as visualized using SDS-PAGE and fluorescence microscopy. This knowledge is important for future application of Kdo-8-N_3 in the study of LPS biosynthesis and dynamics, especially when working with clinical isolates.

Introduction

The Gram-negative bacterial cell envelope is a crucial structure that plays an important role in maintaining cellular integrity, but is also a protective barrier against external stress, a regulator of nutrient uptake and involved in host–pathogen interactions.[1] Important for bacterial cellular integrity is the production of membrane-bound lipopolysaccharides (LPS). LPS generally function as the first defense layer against environmental stress and preserve the structural integrity of the bacterial cell envelope found in virtually all Gram-negative bacteria.[2] LPS consist of three main parts: (1) a lipophilic region, lipid A, that is embedded into the membrane, (2) a core oligosaccharide region attached to lipid A, that further divides into inner core and outer core, and (3) *O*-antigen, a highly diverse polysaccharide chain that is linked to the core region and extends out of the cell surface. The length and structure of LPS highly varies among Gram-negative bacterial strains, and even among serotypes, mostly due to the variety of carbohydrates on the outer core and *O*-antigen regions. However, in almost all Gram-negative bacteria the contents of lipid A and inner core regions are highly conserved with only small variations to the length and position of lipid chains.

3-Deoxy-D-*manno*-oct-2-ulosonic acid (Kdo), a bacteria-specific anionic monosaccharide composed of an eight-carbon backbone, is part of the inner core region of LPS and is specifically responsible for linking the inner core region to lipid A. Due to its unique position and highly conserved presence in the core of LPS, Kdo is thought of as a marker for LPS formation.[2,3] Kdo has an anionic character that increases the strength of neighboring LPS interactions and lowers the permeability of the outer membrane that acts as a protective barrier against foreign compounds.[4,5] In *Escherichia coli* strains, the smallest structure of LPS that still allows cellular growth and viability has been found to contain two Kdo residues linked to lipid A.[2] This structure, known as Kdo_2-lipid A, is a widespread motif among bacterial LPS structures, although a structure with only one Kdo unit attached to lipid A is found in some Gram-negative bacteria such as *Haemophilus influenzae*[6,7] and *Bordetella pertussis*.[8] Because of its key position in the LPS structure, Kdo is considered an attractive monosaccharide to target in the biosynthetic pathway of LPS for the investigation of Gram-negative bacteria and their LPS production.[9]

Gram-negative bacteria employ two biosynthesis methods to produce Kdo-linked LPS: a *de novo* pathway and a salvage

[a] Stratingh Institute for Chemistry, Faculty of Science and Engineering, University of Groningen, Nijenborgh 7, 9747 AG Groningen, The Netherlands. E-mail: m.t.c.walvoort@rug.nl
[b] Department of Medical Microbiology, University of Groningen, University Medical Center Groningen, Hanzeplein 1, 9700 RB Groningen, The Netherlands
[c] Groningen Biomolecular Sciences and Biotechnology Institute, Faculty of Science and Engineering, University of Groningen, Nijenborgh 7, 9747 AG Groningen, The Netherlands

† Electronic supplementary information (ESI) available. See DOI: https://doi.org/10.1039/d3cb00110e

pathway (Fig. S1, ESI†). In the *de novo* pathway, Kdo is produced from ribulose 5-phosphate, which is a product generated from D-glucose through the pentose phosphate pathway, by the action of several enzymes.[10–12] In the Kdo salvage pathway, exogenous Kdo is imported by the sialic acid transporter NanT, which was recently found to be involved in the uptake of Kdo and a derivative of Kdo in *E. coli* cells.[13] The Kdo from either pathway is subsequently activated to its CMP derivative (CMP-Kdo) by CMP-Kdo synthase, and transferred to lipid A by CMP-Kdo transferase (Fig. S1, ESI†).[13]

8-Azido-3,8-dideoxy-α/β-D-*manno*-oct-2-ulosonic acid (Kdo-8-N_3) is a synthetic derivative of the natural compound Kdo that contains an azide moiety on the primary carbon. Several studies have used this modified Kdo substrate to metabolically label LPS in a selection of Gram-negative bacteria (Fig. 1).[9,13–18] Labeling experiments involve the uptake of Kdo-8-N_3 inside the bacterial cytosol, where it is processed to the nucleotide-activated CMP-Kdo-8-N_3 form. Next, Kdo-transferase adds Kdo-8-N_3 to the growing lipid A structure, after which the glycoconjugate is flipped to the extracellular surface. A subsequent click reaction with a fluorescent label allows the visualization of labeled LPS structures using SDS-PAGE gel imaging and fluorescence microscopy on whole cells. In the first account in 2012, Kdo-8-N_3 was chemically synthesized and used as a tool to label LPS and to selectively visualize the cell membrane of *E. coli* K-12, *Salmonella thyphimurium*, and *Legionella pneumophila* strain Paris using fluorescence microscopy.[9] Bacteria were incubated in a minimal medium (M9) with Kdo-8-N_3 and subsequently reacted with a fluorophore through copper-catalyzed click chemistry. This method was further improved by growing the bacterial cells in a richer media (LB) supplemented with lower concentrations of Kdo-8-N_3 and using an intact-cell compatible, strain-promoted click reaction.[13–15] Using this method, Kdo-8-N_3 was also incorporated into LPS in a variety of Gram-negative bacteria, such as an *E. coli* mutant strain that produces highly truncated LPS structures, an *E. coli* mutant strain lacking *de novo* Kdo biosynthesis (*ClearColi* K-12), *E. coli* serotype O6, *Klebsiella pneumoniae* K6, and two antibiotic-resistant *E. coli* strains. Furthermore, the LPS of *Brucella abortus*,[16] *Myxococcus xanthus* DZ2,[17] and of Gram-negative bacteria found in the murine gut microbiota[18] were labeled using different concentrations of Kdo-8-N_3 in various growth media.

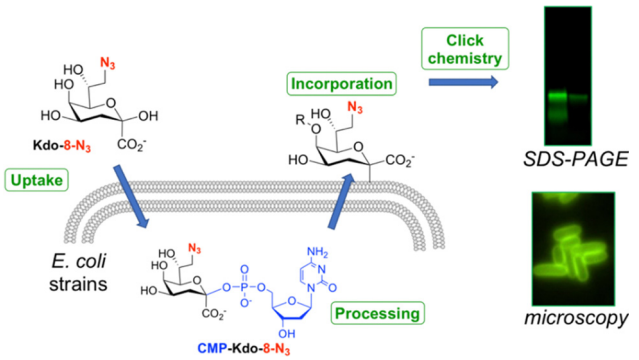

Fig. 1 Overview of the method of fluorescent LPS labeling used in this work.

Whereas successful incorporation of Kdo-8-N_3 into the LPS was reported in several Gram-negative bacteria, it has been estimated that the efficiency of Kdo-8-N_3 incorporation is <1% compared to native Kdo, which may be caused by low uptake or poor efficiency of the 8-azido analogue in the enzymatic processing steps.[9,14] To increase uptake efficiency, minimal media (*e.g.*, M9 medium) are often used to introduce unnatural carbohydrate analogues, as this was shown to stimulate carbohydrate uptake.[19] On the other hand, growth in rich media (*e.g.* LB medium) is also able to support analogue incorporation.[20] Because we anticipate that Kdo-8-N_3 will be widely used and very useful for the study of bacterial LPS and membranes in general,[21] we are convinced it is important to understand under which conditions Kdo-8-N_3 labeling is most likely achieved, and how to best check for successful incorporation.

In this study, the efficiency and reproducibility of the Kdo-8-N_3 labeling method is investigated as a tool to visualize LPS in Gram-negative bacteria, focusing on *E. coli* strains. The method of Kdo-8-N_3 incorporation into LPS was reproduced and optimized for the non-pathogenic *E. coli* K-12 strain (*E. coli* BW25113), followed by the incorporation of Kdo-8-N_3 in a collection of 15 pathogenic *E. coli* strains from commercial and clinical origin. Labeled LPS was visualized using gel electrophoresis (SDS-PAGE) and fluorescence microscopy. Our findings show that the efficiency of Kdo-8-N_3 incorporation and subsequent labeling of LPS is highly dependent on both the specific strain of bacteria and the growth medium.

Results

Chemical synthesis of Kdo and Kdo-8-N_3

Kdo (**1**) was synthesized using the reported method for the synthesis of ammonium Kdo by Kosma *et al.*[22] (Fig. 2). The two-step synthesis consisted of the aldol reaction between commercial D-arabinose and oxaloacetate at pH 12, followed by decarboxylation with $NiCl_2$ at pH 5 and 50 °C to yield Kdo (**1**). The synthesis of Kdo-8-N_3 (**4**) followed a similar synthetic protocol. For this, 5-azido-5-deoxy-D-arabinose (**3**: Ara-5-N_3) was synthesized from commercial D-arabinose in a straightforward manner in just 4 steps (Fig. 2). The methyl acetal of D-arabinose (**S1**) was synthesized to lock the ring in the 5-membered conformation, followed by iodination of the primary alcohol to give compound **2**. Subsequent azide substitution was followed by acetal hydrolysis to give Ara-5-N_3 (**3**) in 40% yield over 4 steps. Next, compound **3** was subjected to the aldol reaction with oxaloacetate and decarboxylation to obtain Kdo-8-N_3 (**4**) in 80% yield after purification by anion exchange chromatography.

Investigation of growth of *E. coli* BW25113 in the presence of synthetic Kdo and Kdo-8-N_3

We started our investigation into the incorporation efficiency of Kdo-8-N_3 into LPS by assessing the effect of Kdo or Kdo-8-N_3 supplementation on bacterial growth rates in different media.

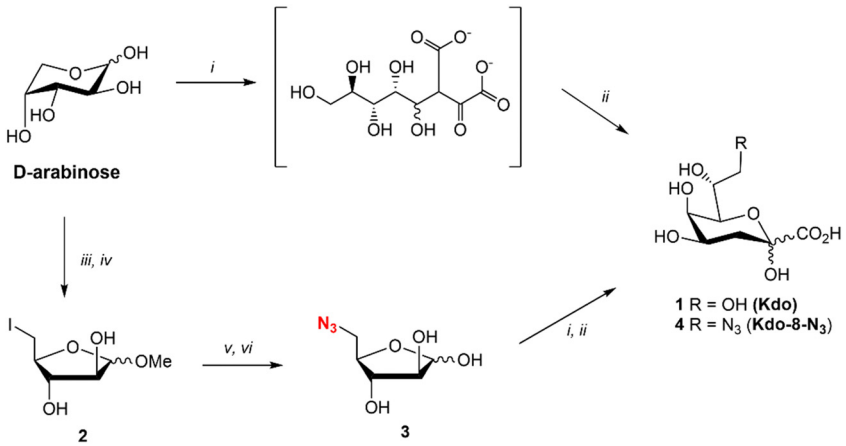

Fig. 2 Synthesis of Kdo (**1**) and Kdo-8-N_3 (**4**). *Reagents and conditions*: (i) oxaloacetate, $NaHCO_3$, NaOH, H_2O, pH 12, rt; (ii) $NiCl_2$, Amberlite-H^+, pH 5, 50 °C (**1** : 36%, **4** : 80%); (iii) 0.18 N HCl in MeOH, 0 °C to rt, 20 h; (iv) I_2, imidazole, PPh_3, THF, 0 to 65 °C, 20 h (56% over two steps); (v) NaN_3, DMF, 80 °C, 20 h; (vi) Amberlite-H^+, H_2O, pH 4, 60 °C, 20 h (72% over two steps).

We selected *E. coli* BW25113 as a benchmark *E. coli* strain, as it has been used to investigate the incorporation of Kdo-8-N_3 into LPS.[14] Because the strain is derived from the non-pathogenic K-12 strain, the LPS is severely truncated and lacks the *O*-antigen and part of the core oligosaccharide region.[12,23] An overnight culture of *E. coli* BW25113 was used to inoculate rich lysogeny broth (LB) medium or minimal medium M9 (containing maltose as carbon source) with or without the supplementation of 5 mM Kdo or 5 mM Kdo-8-N_3. M9 is a chemically defined medium with the minimal nutrients and salts that still allow the majority of bacteria to be viable and replicate.[24] As seen from the growth curves in Fig. 3, the growth of *E. coli* BW25113 in the presence of Kdo or Kdo-8-N_3 in LB is faster (OD_{600} of 0.669 after only 5 hours) and reaches a higher OD_{600} at stationary phase compared to when these substrates were absent from the media. On M9 medium growth was slower and cultures reached a lower OD_{600} at stationary phase (OD_{600} of 0.571 after 12 hours), but in this case the presence of Kdo and Kdo-8-N_3 resulted in faster growth and again, a higher OD_{600}. Interestingly, Kdo-8-N_3 in M9 medium seemed to stimulate bacterial growth more than Kdo in M9 medium. To assess whether the increased growth in the presence of both Kdo and Kdo-8-N_3 could be due to residual pyruvate, we determined the presence of pyruvate using quantitative NMR (qNMR). From the qNMR spectra, 11 mol% and 4 mol% residual pyruvate was determined for the Kdo and Kdo-8-N_3 samples, respectively. As this does not explain the faster growth observed with Kdo-8-N_3 especially, a possible catabolic mechanism for the exogenous Kdo and Kdo-8-N_3 could be present in the cells.

Kdo-8-N_3 labeling and localization on the cell membrane of *E. coli* BW25113

Having established that *E. coli* BW25113 grow well on media supplemented with synthetic Kdo-8-N_3, the incorporation of Kdo-8-N_3 into the cellular LPS was investigated. An overnight culture of *E. coli* BW25113 cells was used to inoculate fresh M9 medium supplemented with or without 5 mM Kdo-8-N_3 and culturing was continued for 16 h. The cells were pelleted, washed and subsequently treated with fluorescein-dibenzocyclooctyne (FAM-DBCO), a strain-promoted fluorescent click reagent that is compatible with intact cells.[25] In accordance with previous reports,[9,14] fluorescence microscopy revealed a

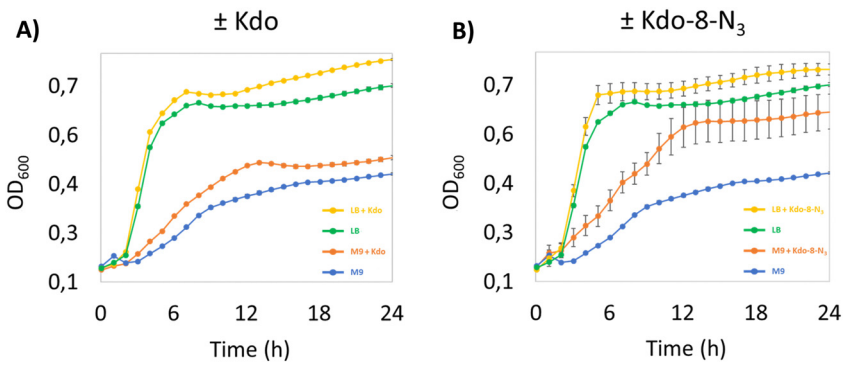

Fig. 3 *E. coli* BW25113 grown in; (A): LB or M9 media with or without 5 mM Kdo. (B): LB or M9 media with or without 5 mM Kdo-8-N_3. OD_{600} values were obtained by growing the bacteria in microtiter 96-well plates and measuring OD_{600} on a microtiter plate reader over 24 h. Values are calculated from triplicates and the average values are displayed. Error bars indicate standard deviations.

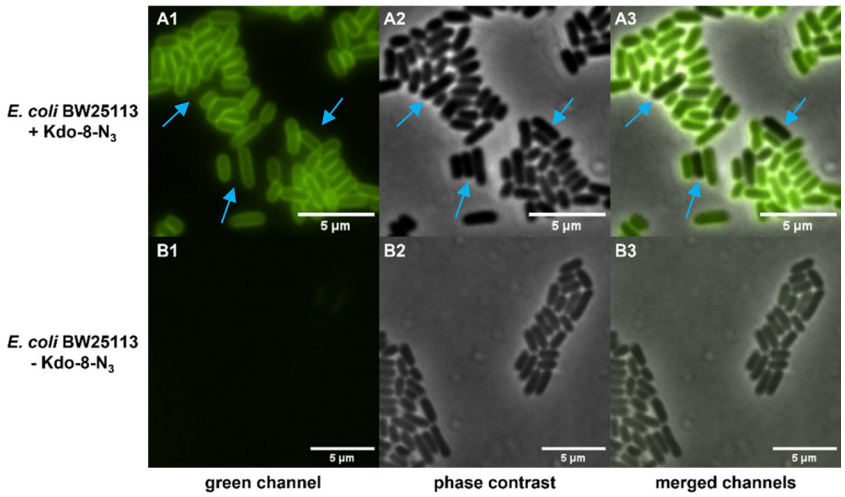

Fig. 4 Kdo-8-N_3 is labeled on the circumference of *E. coli* BW25113 cells. Cells were visualized on a Nikon Ti-E microscope using fluorescence optics (A1, B1: green channel), phase contrast (A2, B2), and co-localization of fluorescent and phase contrast images (A3, B3: merged channels). While *E. coli* cells supplied with Kdo-8-N_3 show green fluorescence signal localized on the periphery of the cell (A panels), *E. coli* cells grown without the presence of Kdo-8-N_3 show no peripheral fluorescence (B panels).

strong fluorescent signal localized to the cell membranes of *E. coli* BW25113 cells when grown with Kdo-8-N_3 (Fig. 4). As a control, no fluorescence signals were observed when the bacteria were grown with 5 mM Kdo, or when the click reagent was omitted (Fig. S2, ESI†). Interestingly, a number of cells was observed to have no labeling at all (Fig. 4; panel A3: indicated by blue arrows), suggesting heterogeneity in the bacterial culture at the time of incubation with Kdo-8-N_3. Bacterial culture heterogeneity has been described for *E. coli* cells as a result of the dilution of cells in stationary phase.[26]

Confirmation by SDS-PAGE of Kdo-8-N_3 incorporation into *E. coli* BW25113 LPS

To verify that the fluorescent signal localized to the periphery of *E. coli* BW25113 cells upon incubation with Kdo-8-N_3 actually originates from labeled LPS, 16% Tris-Tricine SDS polyacrylamide gel electrophoresis (PAGE) was used to separate and visualize LPS. The bands were visualized using fluorescence imaging (Fig. 5A), and total LPS was visualized both with the Pro Q Emerald 300 LPS gel staining kit (Fig. 5B: UV-B visible) and with silver staining (Fig. 5C). To confirm that the observed labeling on the LPS structures originated from incorporation of the chemically synthesized Kdo-8-N_3 (compound **4**), the experiment was repeated with commercial Kdo-8-N_3 (>90% purity), and the resulting gels were visualized using fluorescence imaging (Fig. 5E) and with silver staining to reveal total LPS (Fig. 5F). Commercial LPS from *E. coli* O55:B5 and commercial Kdo_2-lipid A were used as a reference. In addition, Coomassie staining was performed to exclude the presence of proteins on the SDS-PAGE images (Fig. S3, ESI†).

Fluorescent LPS bands were observed in the cells grown with Kdo-8-N_3 (Fig. 5A, lanes 4, 5, 6, 7). These fluorescent bands were absent from the cells grown without Kdo-8-N_3 (lanes 8 and 9), indicating that the fluorescent labeling of LPS is Kdo-8-N_3-dependent. The highest fluorescence intensity was observed with the samples containing cells grown in the presence of 5 mM Kdo-8-N_3, and LB and M9 media both gave bands with reliable fluorescence intensity (lane 5 and 7). The fluorescent signal was slightly more intense with the growth in LB (lane 7). Interestingly, a similar pattern of fluorescence intensity was observed when the commercial Kdo-8-N_3 was used (Fig. 5E and F), suggesting that both compound **4** and the commercial Kdo-8-N_3 were equally efficient in LPS labeling. The two methods for total LPS staining showed identical LPS patterns (Fig. 5B and C), including two distinct bands with similar molecular weights, which had a lower mobility on SDS-PAGE than Kdo_2-lipid A (Fig. 5, lane 3). This suggests that *E. coli* BW25113 produces at least two LPS structures that contain several monosaccharides additional to Kdo_2-lipid A (core-lipid A or rough LPS). This observation is in agreement with reported results that showed a clear difference in molecular weight between the short chain LPS of *E. coli* BW25113 and the deep-rough LPS of a genetically engineered Δ*waaC E. coli* strain that only produces Kdo_2-lipid A.[14] The superimposed image (Fig. 5D) revealed that the fluorescently labeled LPS structures (red bands) match the higher band of the LPS structures (green bands). This result shows that Kdo-8-N_3 is incorporated into the LPS structures on the bacterial cell envelope, which was previously confirmed by MALDI-TOF MS studies.[14] Comparison of the two LPS visualization methods showed that both revealed the same LPS pattern, but that the silver stain protocol showed a greater signal-to-background ratio than the commercial Pro Q Emerald 300 LPS gel staining kit.

Therefore, the LPS-specific silver stain protocol was used for the ensuing experiments.

Fluorescent labeling of *E. coli* BW25113 with Kdo-8-N_3 and different click reagents

To optimize the fluorescence read-out and to understand if the LPS visualization is fluorophore-dependent, three strain-promoted click reactions (copper-free) and one copper-catalyzed click reaction

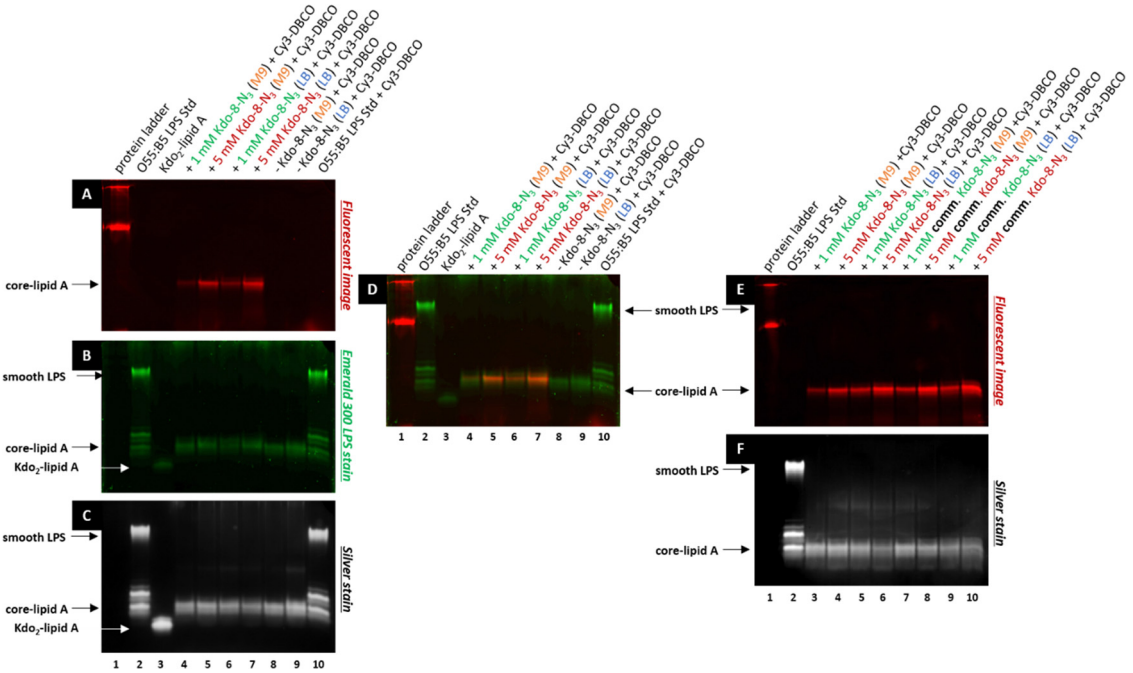

Fig. 5 Total LPS was separated on 16% Tris-Tricine SDS-PAGE and the labeled bands were visualized under fluorescence. *E. coli* BW25113 cells grown with or without Kdo-8-N_3 (1 mM or 5 mM) in M9 minimal medium or the rich LB medium and 'clicked' with Cy3-DBCO; (A): fluorescence image taken in the red channel. (B): Gel imaged with UV-B (300 nm) illumination after staining with the Emerald 300 gel LPS staining kit. (C): Gel scanned after silver staining protocol. (D): Superimposed images of the fluorescent gel (panel A) and after staining with Pro Q Emerald 300 LPS staining kit (panel B). A comparison between the chemically synthesized Kdo-8-N_3 (compound **4**) and commercial Kdo-8-N_3 revealed similar incorporation efficiency. (E): Fluorescence image taken in the red channel. (F): Gel scanned after silver staining protocol.

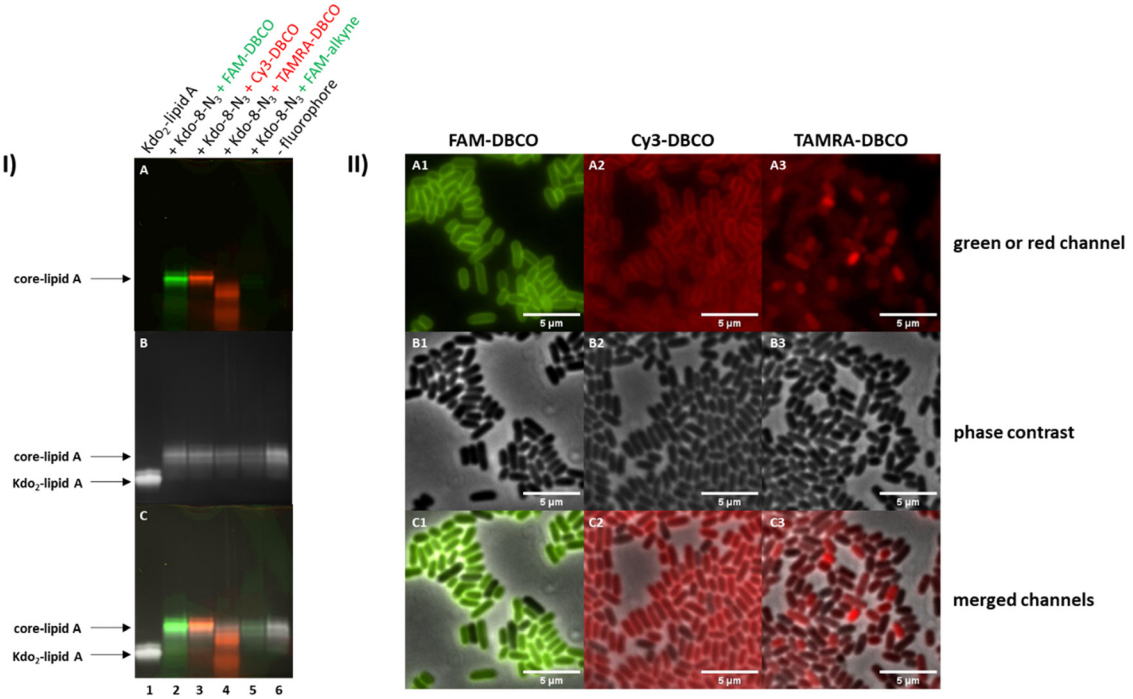

Fig. 6 (I): Fluorescent bands and total LPS visualized on 16% Tris-Tricine SDS-PAGE images: (A) fluorescence image showing FAM-DBCO, Cy3-DBCO, TAMRA-DBCO and FAM-alkyne labeling on LPS. (B) Total LPS visualized by silver staining. (C) Superimposed images of fluorescent and silver-stained gels showing the match/mismatch of labeled LPS structures. (II): Microscopy images showing peripheral labeling by strain-promoted click reactions with FAM-DBCO, Cy3-DBCO, and nonselective labeling of cellular compounds with TAMRA-DBCO.

with different fluorophores were investigated. *E. coli* BW25113 cells were grown in M9 medium with the supplementation of Kdo-8-N_3 (5 mM) and treated with fluorescein (FAM)-DBCO, cyanine-3 (Cy3)-DBCO, carboxytetramethylrhodamine (TAMRA)-DBCO and FAM-alkyne. The 16% Tris-Tricine SDS-PAGE gel images in Fig. 6-I show that the highest amount of labeling was observed with FAM-DBCO and Cy3-DBCO. Labeling with TAMRA-DBCO seems to be restricted to non-LPS material (see superimposed image, panel I-C). The copper-catalyzed click reaction resulted in a very faint band on the gel image (Fig. 6-I: A, lane 5), which we hypothesize is due to loss of LPS as a result of cell lysis or membrane damage during the incubation with copper,[27–29] as the amounts of LPS after copper-catalyzed click reactions were generally lower. To reduce potential toxicity, the copper-catalyzed click reaction may be improved by further optimizing the copper to ligand ratio, or by the use of alternative ligands such as BTTP and BTTAA.[29,30] However, as the strain-promoted click reactions were successful, this was not pursued in this project.

The differences in fluorescence intensity observed on the Tricine gels were consistent with observations made using fluorescence microscopy (Fig. 6-II). The strain-promoted reactions with FAM-DBCO and Cy3-DBCO resulted in clear peripheral labeling of *E. coli* BW25113 cells (A1 and A2 respectively), which was not observed with TAMRA-DBCO (A3). The cells labeled using the copper-catalyzed reaction with FAM-alkyne were not included in the microscopy experiments due to the low level of fluorescence intensity (Fig. 6-I: A, lane 5). As FAM-DBCO-labeled cells (Fig. 6-II: A1) show brighter labeling than Cy3-DBCO-labeled cells, we concluded that FAM-DBCO was the best fluorophore for future experiments.

Effect of growth media on the incorporation of Kdo-8-N_3 into LPS of pathogenic *E. coli* strains

Having established that Kdo-8-N_3 is successfully incorporated into the LPS of the non-pathogenic *E. coli* BW25113 strain, we set out to assess the generality of this approach to label different *E. coli* serotypes and clinical isolates. For this, a selection of pathogenic *E. coli* strains containing different LPS patterns was used (Table S1, ESI†): *E. coli* O55:B5 (commercial strain), *E. coli* O119 (commercial strain), *E. coli* ET8 (engineered strain), and clinical *E. coli* isolates from blood and implant infections. On *E. coli* BW25113 the largest extent of labeling was observed using 5 mM Kdo-8-N_3, and LB and M9 media both gave reliable fluorescent signals, with the growth in LB resulting in slightly more intense bands.

Each pathogenic *E. coli* strain was incubated with 5 mM Kdo-8-N_3 in either LB or M9 media, followed by the FAM-DBCO click reaction, separation using 16% Tris-Tricine SDS-PAGE and visualization of the bands using fluorescence scanning and silver staining (Fig. 7). The cell density in each well was normalized to ensure comparability between lanes. As is apparent from Fig. 7A, only two out of fifteen pathogenic *E. coli*

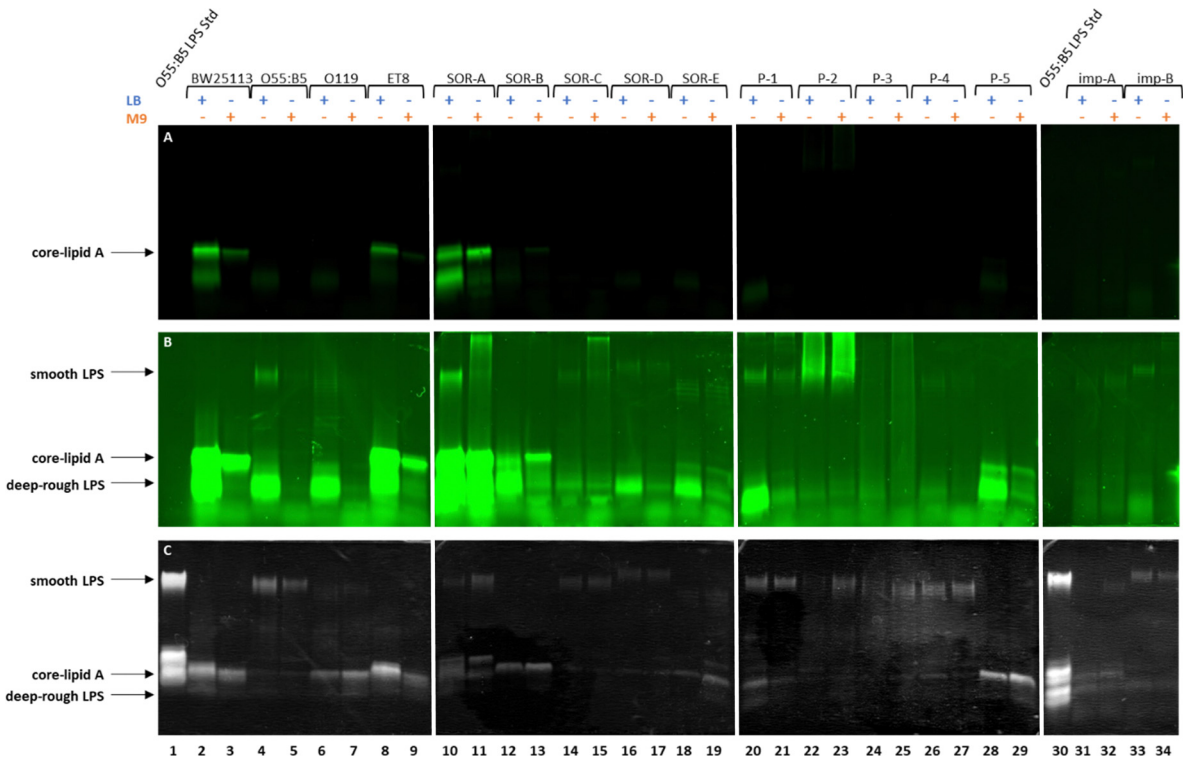

Fig. 7 Labeled LPS bands and total LPS visualized on 16% Tris-Tricine SDS-PAGE images: (A) fluorescence gel image showing the labeling of the LPS in different *E. coli* strains grown in either M9 or LB media supplemented with 5 mM Kdo-8-N_3. (B) Image of panel A shown with enhanced fluorescence intensity. (C) Silver-stained gel image showing the total LPS of the different *E. coli* strains. Each lane is labeled with the name of the *E. coli* strain and the media used. The plus (+) sign indicates the medium used for cell growth.

strains showed a similar extent of labeling at the core-lipid A region compared to *E. coli* BW25113. These strains were *E. coli* ET8 (lanes 8,9) and *E. coli* SOR-A (lanes 10,11). Using the imaging software, the fluorescence intensity was manually increased to view labeled LPS bands with lower intensity which revealed additional fluorescent bands in the low molecular weight region for almost all strains (Fig. 7B). For some of the strains (*i.e.* SOR strains, P-1 and P-5), these bands, which were most apparent when grown in LB, indicated a smaller LPS structure (deep-rough LPS). To better understand these structures, commercial Kdo_2-lipid A was added as a reference on the next gel (Fig. S4, ESI†). Although these bands seem to be similar in size to Kdo_2-lipid A, it is unclear why these bands do not stain well with silver. Using the silver stain (Fig. 7C), it was shown that several strains produce high molecular weight LPS structures (smooth LPS), and also low levels of fluorescent labeling were discernable by increasing the intensity (Fig. 7B). A striking observation was the variety of the labeled LPS patterns within the strains grown in different media. For example, both the labeling efficiency and the labeled LPS pattern of *E. coli* SOR-A differed when grown in LB or in M9 (Fig. 7A and B, lanes 10 and 11). Furthermore, *E. coli* ET8 and SOR-B seemed to label more efficiently when grown in M9 as compared to LB. Overall, the silver-stained gel images nicely illustrate the structural differences in LPS between the investigated *E. coli* strains.

Effect of Kdo substrate on the LPS structures

The labeling experiment revealed that different *E. coli* strains incorporated Kdo-8-N_3, with varying efficiency, which was also impacted by the growth media. To investigate whether Kdo-8-N_3 also impacted the size or the abundance of LPS structures, the LPS pattern of each *E. coli* strain grown in LB supplemented with 5 mM Kdo-8-N_3, 5 mM Kdo, or no additional substrate (negative control) was determined. As visualized in Fig. 8, diverse effects on the LPS production in each individual strain were observed. When supplied with exogenous Kdo, some strains seemed to display reduced amounts of smooth LPS (*i.e.*, O55:B5, SOR-A, SOR-B, SOR-C, SOR-D, P-1), whereas other strains seemed to produce even more smooth LPS (P-2, P-3). Interestingly, Kdo supplementation stimulated the production of short chain (rough) LPS in most of the strains. In contrast, in almost all strains Kdo-8-N_3 supplementation resulted in a reduction in shorter chain LPS. The most striking differences in LPS production were observed between *E. coli* strains SOR-A and SOR-B. When supplied with Kdo-8-N_3, LPS levels were low in SOR-A compared to when grown without any additional substrate, whereas short chain LPS levels were increased when supplied with Kdo. The LPS pattern of SOR-B grown in LB media revealed several bands corresponding to various short-chain LPS structures, however when supplied with Kdo or Kdo-8-N_3, only a single short chain LPS structure was abundantly present. These observations suggest that the LPS biosynthesis in individual strains is impacted by the supplementation of exogenous Kdo and Kdo-8-N_3, and that each strain responds differently to the presence of these substrates.

Localization of labelled Kdo-8-N_3 on pathogenic *E. coli* strains

The results obtained with the pathogenic *E. coli* strains indicated variable Kdo-8-N_3 incorporation into both rough and smooth LPS. To determine whether the labeled LPS structures in these strains are indeed peripherally localized on the cells, a selection of the labeled strains was visualized with microscopy. The LPS of *E. coli* SOR-A had shown intense fluorescent labeling to a comparable extent as *E. coli* BW25113 (Fig. 7A and B), and indeed peripheral fluorescence was observed when the cells were grown in LB or M9 medium (Fig. 9). This suggests that the different patterns for LPS labeling (Fig. 7) both lead to efficient membrane labeling. In the *E. coli* SOR-B samples, only few cells revealed membrane labeling. The periphery of these cells was more apparent for the cells grown in M9, in agreement with the gel electrophoresis data that showed more pronounced labeling in M9 (Fig. 7A). Surprisingly, no labeling was observed in the samples containing *E. coli* O55:B5 cells. While *E. coli* O55:B5 had shown labeling of smooth LPS on the gel images (Fig. 7A), the extent of labeling was probably too low to detect by fluorescence microscopy.

Discussion

In the last decade, Kdo-8-N_3 attracted increasing attention due to several reports on its successful incorporation into the LPS of a variety of Gram-negative bacteria. It allowed selective labeling of living bacteria and was mainly used for imaging purposes.[31]

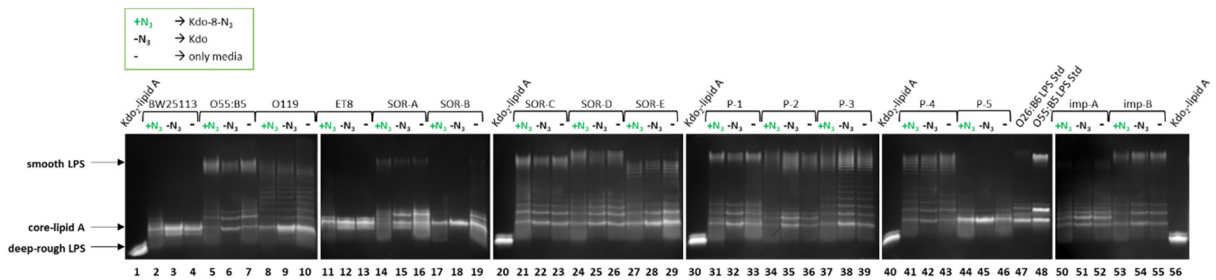

Fig. 8 Silver-stained 16% Tris-Tricine SDS-PAGE gels showing the variety of LPS structures between different *E. coli* strains when grown in LB with 5 mM Kdo-8-N_3 (+N_3), with 5 mM Kdo (−N_3) or without the supplementation of either substrate (−). See Fig. S4 (ESI†) for fluorescence and merged images of these gels.

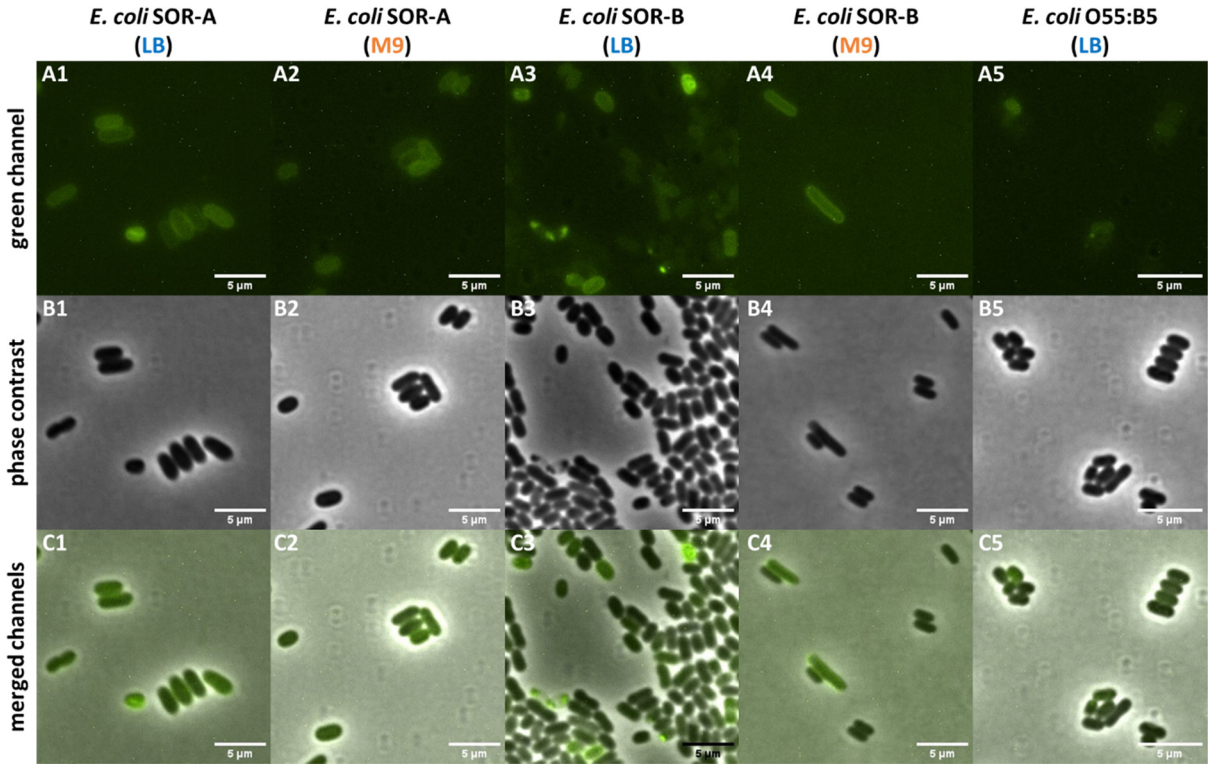

Fig. 9 Selected pathogenic *E. coli* cells visualized on a Nikon Ti-E microscope using fluorescence optics (A1–A5: green channel), phase contrast (B1–B5), and co-localization of fluorescence and phase contrast images (C1–C5: merged channels). All fluorescent images were adjusted to the same settings (*i.e.* brightness, contrast) to allow visualization of different fluorescence intensities of the samples. See Fig. S5 (ESI†) for the control images for LPS labeling using SDS-PAGE.

Triggered by the large potential for employing this Kdo derivative in understanding LPS biosynthesis and dynamics, in real time and under varying conditions, we set out to investigate the generality of the labeling approach across a diverse selection of commercial and clinical strains. Surprisingly, while all included strains belonged to the species *E. coli*, we observed strong variation in the incorporation of Kdo-8-N_3.

When *E. coli* BW25113 was supplied with either Kdo or Kdo-8-N_3, an increase in growth rate was observed in both media, as compared to the controls where the only carbon source was either amino acids (LB) or maltose (M9). This effect was more pronounced when grown in minimal media (M9). A possible explanation of this positive effect on growth is that *E. coli* BW25113 is able to metabolize Kdo and its 8-azido derivative more readily than maltose. Indeed, several bacterial strains, including *E. coli*, are found to express an enzyme called Kdo-aldolase (EC 4.1.2.23), which catalyzes the retro-aldol reaction to form pyruvate and D-arabinose.[32,33] The full genome of *E. coli* BW25113 has been sequenced, and although there is no Kdo aldolase annotated, various putative aldolases are indicated.[34] Additionally, a catabolic mechanism for sialic acid, a monosaccharide that is closely related to Kdo in structure, has been reported in Gram-negative bacteria.[35] This suggests that the enzymes involved in the sialic acid catabolism may also recognize and catabolize the excess Kdo and Kdo-8-N_3 that is taken up by the bacteria. Alternatively, minor amounts of pyruvate that originate from the chemical synthesis of Kdo and Kdo-8-N_3 may be used as a carbon source and increase growth rates.

In our experiments we found that the growth media used for the bacterial exposure to Kdo-8-N_3 had an impact on the extent of incorporation. With *E. coli* BW25113, it was clear that the cells grew slower in M9 as compared to LB. The pathogenic *E. coli* strains used here exhibited a similar growth rate and pattern based on the OD_{600} measurements after incubation for several hours (data not shown). For the subsequent visualization of LPS production and Kdo-8-N_3 incorporation the cell density was normalized, as this allowed a direct comparison of the effect of growth media (Fig. 7). Variations in LPS levels and Kdo-8-N_3 incorporation were observed for some strains, whereas others seemed not to be affected, and a positive effect could be discerned for both LB and M9. We hypothesize that the expression levels of biosynthetic enzymes play a large role in the levels of LPS production and that the extent of azide incorporation may be dependent on the respective enzyme levels. In contrast to the hypothesis of 'starving conditions' to increase carbohydrate uptake, no clear effect of the minimal media on Kdo-8-N_3 incorporation could be observed.

We were intrigued to see that different *E. coli* strains presented very different extents of LPS labeling with Kdo-8-N_3. Almost all strains showed low-level labeling of an LPS structure that is similar in size to core-lipid A. In addition, a few strains (*i.e.* SOR-A, P-1, P-5) showed labeling of an LPS structure that in

size resembles the deep-rough LPS structures, which have been successfully labeled before.[9,14] And most notably, clinical isolates P-1 and P-2 seemed to incorporate Kdo-8-N_3 in their smooth LPS structures to some extent. As also apparent from the differences in LPS structures and molecular weights observed across our collection of *E. coli* strains (Fig. 8), the chemical diversity of LPS is tremendous.[12]

Finally, we selected several strains that showed some extent of fluorescent labeling on SDS-PAGE for additional microscopy experiments, and were able to demonstrate LPS labeling on the peripheral membrane of the clinical isolates SOR-A and SOR-B. No labeling could be observed with the commercial strain O55:B5, which indeed already showed very faint labeling on SDS-PAGE, where mostly LPS structures of similar weight to Kdo_2-lipid A were visible. This convincingly shows that the fluorescently labeled bands that are visible on SDS-PAGE are indeed LPS structures that are localized to the bacterial cell membrane.

Conclusions

Kdo-8-N_3 holds great promise as a tool to selectively visualize the production and dynamics of the LPS of Gram-negative bacteria. We conclude that our understanding of LPS labeling may be improved by performing a screen of different growth media. In addition, we propose that it is crucial to prove the efficiency of Kdo-8-N_3 incorporation into LPS using SDS-PAGE and fluorescence microscopy, if possible, for any bacterial strain of interest, and to optimize the method where necessary. As fluorescent labeling was found to vary greatly between different *E. coli* strains, a thorough validation of Kdo-8-N_3 incorporation prior to embarking on functional studies will be instrumental for the applicability of this method for LPS labeling.

Author contributions

Z. S. Z., M. T. C. W. and D.-J. S conceived and designed the study. Z. S. Z. performed the chemical synthesis, labeling experiments, and imaging. G.-J. P. contributed to the chemical synthesis. M. R. contributed to the labeling experiments. J. M. D. contributed the clinical isolates. Z. S. Z. and M. T. C. W. wrote the manuscript. All authors approved the final version.

Conflicts of interest

There are no conflicts to declare.

Acknowledgements

We thank F. M. Cavallo, L. M. Braams and G. B. Spoelstra at the University Medical Center Groningen for their help with the isolation and culturing of clinical *E. coli* isolates. This work was financially supported by the Faculty of Science and Engineering, University of Groningen.

References

1 T. J. Silhavy, D. Kahne and S. Walker, *Cold Spring Harb. Perspect. Biol.*, 2010, **2**, a000414.
2 C. Erridge, E. Bennett-Guerrero and I. R. Poxton, *Microbes Infect.*, 2002, **4**, 837–851.
3 A. Basauri, C. González-Fernández, M. Fallanza, E. Bringas, R. Fernandez-Lopez, L. Giner, G. Moncalián, F. de la Cruz and I. Ortiz, *Crit. Rev. Biotechnol.*, 2020, **40**, 292–305.
4 A. Silipo and A. Molinaro, *Subcell. Biochem.*, 2010, **53**, 69–99.
5 E. Frirdich and C. Whitfield, *J. Endotoxin Res.*, 2005, **11**, 133–144.
6 K. A. White, I. A. Kaltashov, R. J. Cotter and C. R. H. Raetz, *J. Biol. Chem.*, 1997, **272**, 16555–16563.
7 K. A. White, S. Lin, R. J. Cotter and C. R. H. Raetz, *J. Biol. Chem.*, 1999, **274**, 31391–31400.
8 T. Isobe, K. A. White, A. G. Allen, M. Peacock, C. R. H. Raetz and D. J. Maskell, *J. Bacteriol.*, 1999, **181**, 2648–2651.
9 A. Dumont, A. Malleron, M. Awwad, S. Dukan and B. Vauzeilles, *Angew. Chem.*, 2012, **124**, 3197–3200.
10 L. Cipolla, A. Polissi, C. Airoldi, L. Gabrielli, S. Merlo and F. Nicotra, *Curr. Med. Chem.*, 2011, **18**, 830–852.
11 C. R. H. Raetz, C. M. Reynolds, M. S. Trent and R. E. Bishop, *Annu. Rev. Biochem.*, 2007, **76**, 295–329.
12 C. R. H. Raetz and C. Whitfield, *Annu. Rev. Biochem.*, 2002, **71**, 635–700.
13 I. Nilsson, R. Prathapam, K. Grove, G. Lapointe and D. A. Six, *Mol. Microbiol.*, 2018, **110**, 204–218.
14 I. Nilsson, K. Grove, D. Dovala, T. Uehara, G. Lapointe and D. A. Six, *J. Biol. Chem.*, 2017, **292**, 19840–19848.
15 E. Fugier, A. Dumont, A. Malleron, E. Poquet, J. M. Pons, A. Baron, B. Vauzeilles and S. Dukan, *PLoS One*, 2015, **10**, 1–15.
16 V. Vassen, C. Valotteau, C. Feuillie, C. Formosa-Dague, Y. F. Dufrêne and X. De, Bolle, *EMBO J.*, 2019, **38**, 1–15.
17 F. Saidi, O. J. Gamboa Marin, J. I. Veytia-Bucheli, E. Vinogradov, G. Ravicoularamin, N. Y. Jolivet, A. A. Kezzo, E. R. Esquivel, A. Panda, G. Sharma, S. P. Vincent, C. Gauthier and S. T. Islam, *ACS Omega*, 2022, **7**, 34997–35013.
18 W. Wang, Y. Zhu and X. Chen, *Biochemistry*, 2017, **56**, 3889–3893.
19 P. Rugbjerg, A. M. Feist and M. O. A. Sommer, *Front. Bioeng. Biotechnol.*, 2018, **6**, 1–6.
20 P. Luong, A. Ghosh, K. D. Moulton, S. S. Kulkarni and D. H. Dube, *ACS Infect. Dis.*, 2022, **8**, 889–900.
21 D. A. C. Heesterbeek, R. M. Muts, V. P. van Hensbergen, P. de Saint Aulaire, T. Wennekes, B. W. Bardoel, N. M. van Sorge and S. H. M. Rooijakkers, *PLoS Pathog.*, 2021, **17**, 1–22.
22 H. Mikula, M. Blaukopf, G. Sixta, C. Stanetty and P. Kosma, *Carbohydr. Chem.: Proven Synth. Methods*, 2015, 207–211.
23 V. Chang, L.-Y. Chen, A. Wang and X. Yuan, *J. Exp. Microbiol. Immunol.*, 2010, **14**, 101–107.
24 Cold Spring Harbor Protocols, 2010, pdb.rec12295.
25 N. J. Agard, J. M. Baskin, J. A. Prescher, A. Lo and C. R. Bertozzi, *ACS Chem. Biol.*, 2006, **1**, 644–648.
26 J. Roostalu, A. Jõers, H. Luidalepp, N. Kaldalu and T. Tenson, *BMC Microbiol.*, 2008, **8**, 1–14.

27 R. Hong, T. Y. Kang, C. A. Michels and N. Gadura, *Appl. Environ. Microbiol.*, 2012, **78**, 1776–1784.
28 P. M. M. Martins, T. Gong, A. A. de Souza and T. K. Wood, *Antibiotics*, 2020, **9**, 1–13.
29 M. Yang, A. S. Jalloh, W. Wei, J. Zhao, P. Wu and P. R. Chen, *Nat. Commun.*, 2014, **5**, 1–10.
30 C. Besanceney-Webler, H. Jiang, T. Zheng, L. Feng, D. Soriano Del Amo, W. Wang, L. M. Klivansky, F. L. Marlow, Y. Liu and P. Wu, *Angew. Chem., Int. Ed.*, 2011, **50**, 8051–8056.
31 N. Banahene, H. W. Kavunja and B. M. Swarts, *Chem. Rev.*, 2022, **122**, 3336–3413.
32 M. A. Ghalambor and E. C. Heath, *J. Biol. Chem.*, 1966, **241**, 3222–3227.
33 B. R. Knappmann and M.-R. Kula, *Appl. Microbiol. Biotechnol.*, 1990, **33**, 324–329.
34 F. Grenier, D. Matteau, V. Baby and S. Rodrigue, *Genome Announc.*, 2018, **2**, e01038–14.
35 E. R. Vimr, K. A. Kalivoda, E. L. Deszo and S. M. Steenbergen, *Microbiol. Mol. Biol. Rev.*, 2004, **68**, 132–153.